ACS APPLIED MATERIALS & INTERFACES

Research Article

www.acsami.org

Toughening of Biodegradable Polylactide/Poly(butylene succinate-*co*-adipate) Blends via in Situ Reactive Compatibilization

Vincent Ojijo,[†,‡] Suprakas Sinha Ray,[†,§,*] and Rotimi Sadiku[‡]

[†]National Centre for Nano-Structured Materials, Council for Scientific and Industrial Research, 1-Meiring Naude Road, Brummeria, Pretoria 0001, South Africa

[‡]Division of Polymer Technology, Department of Chemical, Metallurgical & Materials Engineering, Tshwane University of Technology, Pretoria 0001, South Africa

[§]Department of Applied Chemistry, University of Johannesburg, Doornfontein 2028, Johannesburg, South Africa

[⊥]Department of Chemistry, King Abdulaziz University, Jeddah 21589, Kingdom of Saudi Arabia

ABSTRACT: Polylactide and poly(butylene succinate-*co*-adipate) (PLA/PBSA) were melt-blended in the presence of triphenyl phosphite (TPP). An increase in the torque during melt mixing was used to monitor the changes in viscosity as compatibilization of the blends occurred. Scanning electron micrographs showed not only a reduction in the dispersed-phase size with increased TPP content but also fibrillated links between the PLA and PBSA phases, signifying compatibilization. Moreover, optimization of parameters such as the mixing sequence and time, TPP content, and PBSA concentration revealed that blends containing 30 and 10 wt % PBSA and 2 wt % TPP, which were processed for 30 min, were optimal in terms of thermomechanical properties. The impact strength increased from 6 kJ/m^2 for PLA to 11 and 16 kJ/m^2 for blends containing 30 and 10 wt % PBSA, respectively, whereas the elongation-at-break increased from 6% for PLA to 20 and 37% for blends containing 30 and 10 wt % PBSA, respectively. Upon compatibilization, the failure mode shifted from the brittle fracture of PLA to ductile deformation, effected by the debonding between the two phases. With improved phase adhesion, compatibilized blends not only were toughened but also did not significantly lose tensile strength and thermal stability.

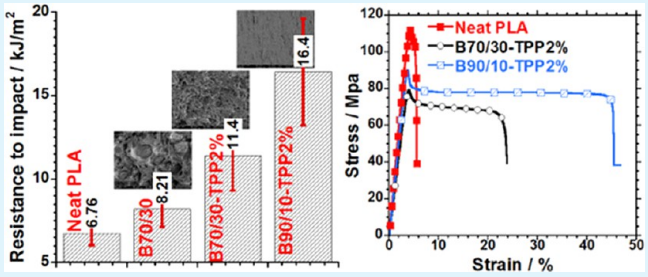

KEYWORDS: *compatibilization, polylactide/poly(butylene succinate-co-adipate) blends, toughening, triphenyl phosphite*

1. INTRODUCTION

Although polylactide (PLA) is a biodegradable polymer with good strength, stiffness, and optical, physical, and barrier properties, its low flexibility[1] (the elongation-at-break for PLA is ∼2.5−6%)[1,2] and low impact strength limit its applications, particularly for packaging industries. Therefore, blending PLA with flexible biodegradable polymers is a practical and economical way to obtain toughened PLA products. The brittleness could be overcome through blending PLA with more ductile biodegradable polymers, such as polycaprolactone (PCL),[3−6] PCL-based random copolymers, e.g., poly(ε-caprolactone-*co*-δ-valerolactone)[7] and poly(ε-caprolactone-*co*-D,L-lactide),[8] poly(butylene adipate-*co*-terephthalate),[9−11] poly(hydroxyalkanoates),[12−14] poly(butylene succinate),[15−17] and poly(butylene succinate-*co*-adipate) (PBSA).[18] However, more often, PLA may not be miscible with some of these polymers, with their blends resulting in phase-separated morphology, which eventually leads to a deterioration in properties. Therefore, various studies have aimed at modifying the morphology to increase the compatibility between the two phases.

In a previous work, the authors melt-blended PLA with PBSA at various compositions and found improvement in properties for samples containing 30 wt % PBSA.[18] However, the strain improved only slightly (from 4 to 6.5%), while the stress/strain curves showed a small ductile failure for this particular blend composition. The argument given for the slight improvement was the maximum specific interfacial area exposed by the PBSA phase for the 70PLA/30PBSA blend, allowing maximum intermingling of PLA and PBSA chains near the interface. In other works, organically modified clays were used to modify the 70PLA/30PBSA blend morphology at different concentrations.[19−21] It was found that 2 wt % loading of organoclay was optimal in improvement of properties. However, for PLA, only a minimal increase in strain of 4−6% was realized. Therefore, even though other properties such as the modulus, strength, and crystallinity either improved or remained constant, the elongation-at-break was not satisfactory. As such, it was deemed necessary to compatibilize PLA and PBSA if improvement in ductility was to be realized.

One way to improve the compatibilized PLA/PBSA blend would be to use copolymers of PLA/PBSA prepared separately,

Received: February 5, 2013
Accepted: April 29, 2013
Published: April 29, 2013

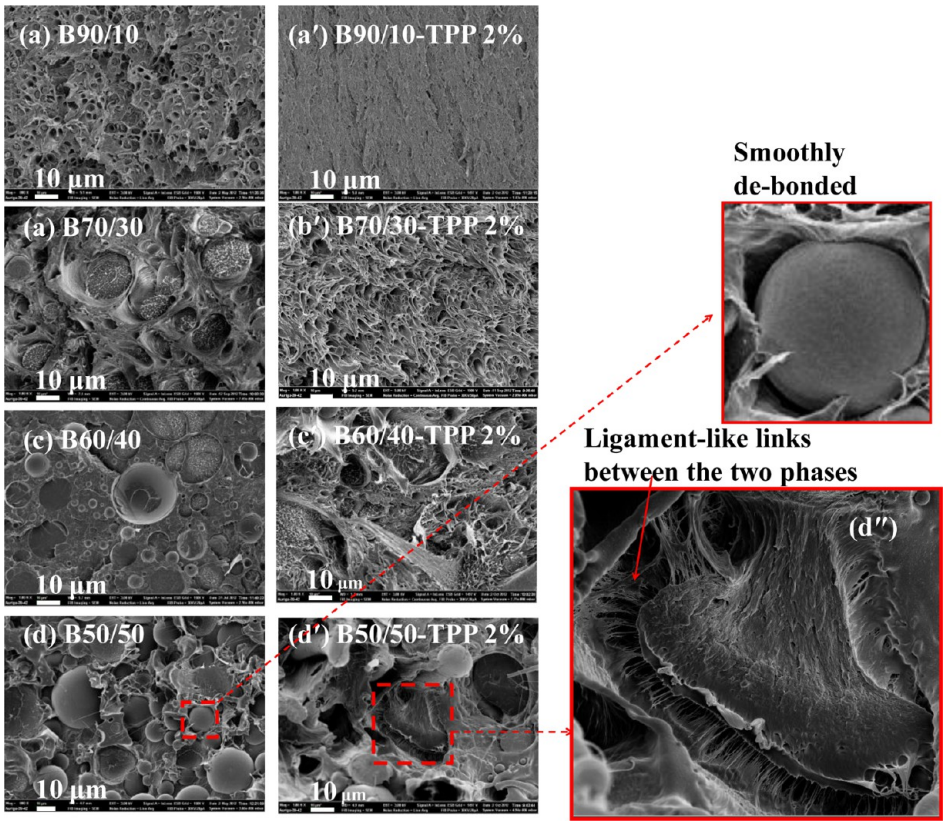

Figure 1. SEM images of neat blends (a–d) and compatibilized blends (a′–d′) of different compositions. A higher magnification of selected sections of parts d and d′ are shown in the inset and part d″, respectively. The presence of ligament-like links between phases in part d″ might be a result of compatibilization. All samples had been annealed at 80 °C for 15 h prior to being subjected to tensile break.

but this would involve an undesirable two-step process. The alternative is to perform a one-step compatibilization process during melt blending. In situ reactive compatibilization is preferred technologically compared to the addition of a specially tailored, usually expensive, copolymer.[22] It has been applied by several authors in compatibilization of PLA with various biodegradable polymers in bids to improve its toughness.[23−25] However, in this work, in situ reactive compatibilization of PLA and PBSA was achieved in the presence of a chain extender, triphenyl phosphite (TPP).

TPP is an ester of phosphonic and phosphorus acids and has a pair of electrons in the phosphorus atom available for reaction with hydroxyl and carboxyl end groups in polymers. As a known chain extender, it has been used by several researchers to increase the molecular weight of poly(ethylene terephthalate) (PET),[26,27] activate transesterification reactions between PET and poly(ethylene naphthalate),[28] and initiate reactive compatibilization of poly(butylene terephthalate) and poly(2,6-dimethyl-1,4-phenylene ether).[22]

Wang et al.[29] used three catalysts/coupling agents in the reactive compatibilization of PLA and PCL: triphenyl phosphate, *p*-toluenesulfonic acid, and dibutyltin dilaurate. For TPP, the elongation-at-break increased from 3% for neat PLA and 28% for the neat 80PLA/20PCL blend to 127% for 80PLA/20PCL with a 2 wt % addition of TPP. The toughening was dependent on the molecular weight of PCL, with the lower-molecular-weight PCL resulting in an elongation-at-break of only 11%. However, among the three coupling agents, TPP resulted in the best improvement in the elongation-at-break, and this formed the basis for its choice in the current work.

To the best of our knowledge, no work has investigated the reactive compatibilization of the PLA/PBSA blend in the presence of any catalyst and/or coupling agent. Therefore, it is the objective of the current study to prepare toughened PLA/PBSA blends in a reactive compatibilization reaction with TPP, characterize them, and relate the morphology to the properties of the blends. This is an important issue in designing PLA-based, environmentally friendly packaging materials.

2. EXPERIMENTAL SECTION

2.1. Materials. PLA used in the study was commercial grade (PLA 2002D) and was obtained from Natureworks, LLC (USA). It had a D-isomer content of approximately 4%, weight-average molecular weight M_w = 235 kg/mol, density = 1.24 g/cm^3, glass transition temperature T_g = ∼60 °C, and melting temperature T_m = ∼153 °C. Conversely, PBSA, with the designation BIONOLLE #3001, was obtained from Showa High Polymer (Japan). According to the supplier, it had M_w = 190 kg/mol, density = 1.23 g/cm^3 (ASTM 1238), T_g = −43.8 °C, and T_m = 83.1 °C (first) and 94.5 °C (second). The coupling agent TPP was obtained from Sigma-Aldrich.

2.2. Preparation of Neat and Compatibilized Blends. Before processing, PLA was dried at 80 °C under vacuum for 36 h, whereas PBSA was dried at 60 °C under vacuum for 12 h. PLA/PBSA blends with various weight ratios were melt-compounded in a HAAKE PolyLab OS Rheomix (Thermo Electron Co., USA) batch mixer operated at a rotor speed of 60 rpm and at a set temperature of 185 °C. Judicious determination of the processing protocol results in a product with optimized properties. The proper mixing of PLA and PBSA before compatibilization is necessary to achieve maximum compatibilization. This was tested by following two processing protocols: (i) PLA and PBSA were melt-blended for 5 min before TPP was added, and the blending was continued for times of 15, 30, and 40 min, depending on the study; (ii) PLA and TPP were melt-

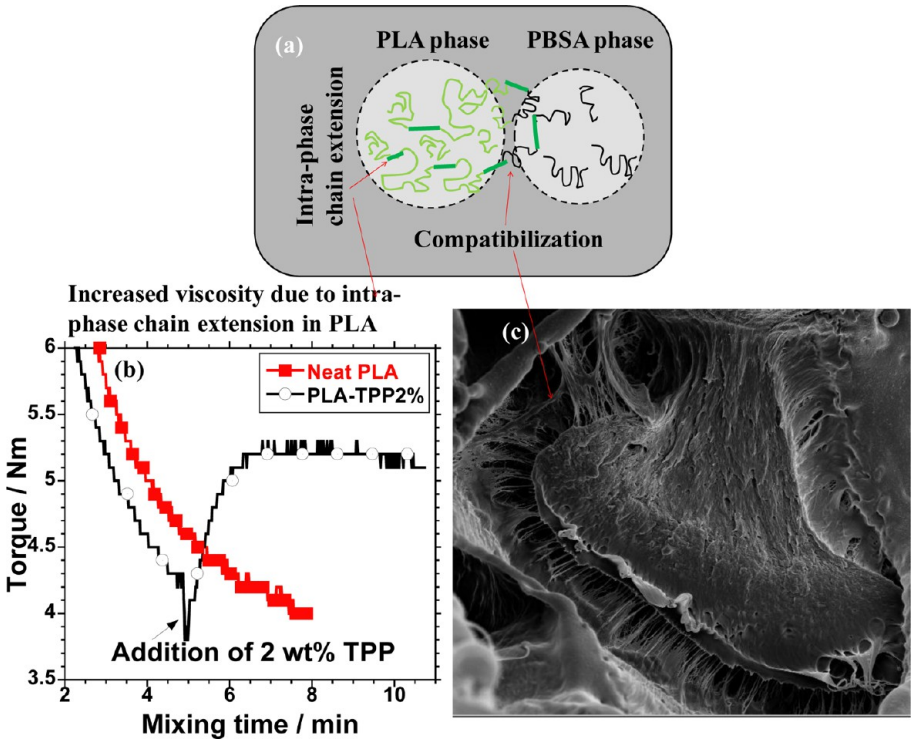

Figure 2. (a) "Cartoon" model depicting intraphase chain extension and interphase compatibilization, (b) torque/time graph for the neat PLA and PLA/TPP2% samples showing intraphase chain extension, and (c) high magnification of the marked section in Figure 1d′.

blended for 3 min, then PBSA was added, and the blending was continued for 12 min. Protocol i yielded samples with slightly better elongation-at-break values (results not shown here) and, hence, was followed for all other sample processing. The blends were then compression-molded into various specimen forms using a Carver laboratory press at 185 °C and cooled to room temperature. To study the effect of crystallinity on the properties of the prepared blends, some samples were not annealed but rather quenched after compression molding. These samples were known as "as-prepared". The prepared blends were coded B*x*/*y*-TPP*z*%, where *x*, *y*, and *z* indicate the percentages of PLA, PBSA, and TPP, respectively.

2.3. Characterization. The surface morphology of the PLA/PBSA blends was studied using scanning electron microscopy (SEM; AURIGA CrossBeamWorkstation from Carl Zeiss) at an accelerating voltage of 3 kV. Dog-bone-shaped samples were annealed at 80 °C for 15 h and subsequently subjected to tensile fracture. The tensile-fractured surfaces were sputter-coated with a gold/palladium alloy to avoid charging (and for possible conduction) before being imaged with SEM.

X-ray diffraction (XRD) analyses of neat and compatibilized PLA/PBSA blends were carried out using a PANanalytical X'pertPRO diffractometer (Cu Kα radiation; λ = 154 nm) operating at 45 kV and 40 mA. Data were obtained from 2θ = 1−70° at a scanning rate of 3.35°/min.

Differential scanning calorimetry (DSC) measurements were carried out on a DSC-Q2000 instrument (TA Instruments) in the temperature range of −65 to +190 °C under a nitrogen atmosphere, using samples of approximately 11.7 mg. The samples were tested at the same heating and cooling rates of 10 °C/min in three scans: heating, cooling, and heating. While the first heating scan erased the previous thermal history of the samples, the second heating scan was used in the determination of T_g, cold crystallization temperature (T_{cc}), T_m, and heat of fusion (ΔH_m). ΔH_m of the PLA component in the first run was used to calculate the crystallinity. Three independent tests were carried out to obtain the average values of T_g, T_{cc}, and the degree of crystallinity.

Thermogravimetric analyses (TGA) were conducted on a TG-Q500 analyzer (TA Instruments). Samples weighing approximately 11 mg were heated from room temperature to 900 °C at a heating rate of 10 °C/min under an air atmosphere. To obtain characteristic thermal stability indicators such as the onset degradation temperature, three independent tests were carried out per sample, and the average value was reported.

Tensile tests to determine the modulus, yield strength, and elongation-at-break were carried out using an Instron 5966 tester (Instron Engineering Corp., USA) with a load cell of 10 kN and according to ASTM 638D standards. This was carried out under tension mode at a single strain rate of 5 mm/min at room temperature. Two dog-bone-shaped sample types were analyzed: (i) "as prepared" without annealing; (ii) annealed at 80 °C for 15 h under vacuum. The results presented are an average of at least six independent tests.

Charpy impact test specimens were compression-molded with dimensions of approximately 80 × 10 × 4 mm ($L \times W \times B$), according to the ISO 179 standard. Specimens were notched on one side, with a notch root radius of 0.25 mm at 2 mm depth using a CEAST Automatic Notchvis Plus (Italy). The notched Charpy impact strength (ISO179) was measured on a fully automated CEAST Pendulum Resil Impactor II (Italy) at room temperature. The drop velocity was 3.7 m/s, with a hammer energy of 7.5 J, and the span between supports was fixed at 40 mm. The results presented are the averages of six independent tests per sample. All of the specimens were annealed at 80 °C for 15 h.

3. RESULTS AND DISCUSSION

3.1. Phase Morphology. The phase morphologies of neat blends of various compositions and their compatibilized counterparts are shown in Figure 1. The blends had been subjected to tensile fracture after annealing at 80 °C for 15 h. The annealing was specifically performed to enable the inferential study of the interfacial adhesion between the two phases because it enhances the separation between them. The neat blends of various compositions had distinct island-sea-type morphologies, indicating poor interfacial adhesion between the phases. This expectedly became worse with increased PBSA

content, as has been discussed in a previous paper.[18] Moreover, there was heterogeneous distribution of the sizes of the dispersed phase. However, the addition of 2 wt % TPP not only reduced the dispersed-phase sizes, causing blends to have uniform morphologies, especially for low PBSA content, but also resulted in a different type of fracture mechanism. The smooth surface of neat blends underwent somewhat brittle failures, while those containing TPP underwent ductile failure, as will be discussed later. This modification of that morphology has been attributed principally to two factors: (i) compatibilization between PLA and PBSA; (ii) alteration of the viscosity as a result of intraphase chain extension during processing.[30]

To support the compatibilization theory, higher-magnification SEM images of blends with 50% PBSA were taken. Higher magnifications of the marked sections of parts d and d′ of Figure 1 are shown in the adjacent images. For the neat 50PLA/50PBSA blend, there were smoothly debonded surfaces, indicating complete phase separation and, hence, brittle fracture. For the 50PLA/50PBSA-TPP2% blend, ligament-like fibrils existed between the two phases, signifying some level of interfacial adhesion, which was a result of compatibilization. This concept is illustrated in the "cartoon" in Figure 2a,c. During reactive processing with TPP, the heterogeneous coupling of PLA and PBSA (chain interchange) leads to the formation of in situ block copolymers, which act as compatibilizers, although unwanted random copolymers may also be formed. It is the copolymers that lead to better interfacial adhesion, resulting in the ligament-like fibrils between phases, as shown in Figure 2a,c.

Likewise, the intraphase chain extension was demonstrated by processing PLA with 2% TPP and monitoring the torque on the extruder for the duration of the processing time as shown in part b of Figure 2. As opposed to the torque of the neat PLA, which continuously decreased with time, the torque of PLA/TPP2% rose after the addition of TPP. This was attributed to the increased viscosity due to chain elongation. Aharoni et al.[26] attributed such an increase in the viscosity when condensation polymers are processed in the presence of TPP to chain extension reactions, resulting in higher molecular weights. Although not shown here, the viscosity of PBSA/TPP2% did not increase, and this was attributed to the already very low viscosity of neat PBSA at the high operating temperature of 185 °C. Because this was significantly above the normal processing temperature of PBSA, degradation may not be ruled out either. Therefore, the increase in the viscosity of PLA contributed to morphology modification by enhancing the deforming stresses during processing, which could then overcome PBSA's restoring stresses from surface tension, thus avoiding coalescence.

The formation of longer chains within the phases and compatibilization of the same at the interfaces led to increases in the viscosities for the blends. Figure 3 shows the tracking of torque during the mixing process for the 70PLA/30PBSA blend with different concentrations of TPP. Unlike determination of the molecular weight, which only takes place after the reaction stops, the torque/time graph allows for dynamic evaluation of the change in viscosity during processing. The PLA/PBSA mixture was melt-blended for 5 min before TPP was added. The increase in TPP led to an increase in the resultant torque after 30 min of mixing, indicating an increase in the viscosity during the processing time. The increase in the viscosity resulted from linkages occurring mostly between PLAs, and to a lesser extent PLA and PBSA, as initiated by TPP and the

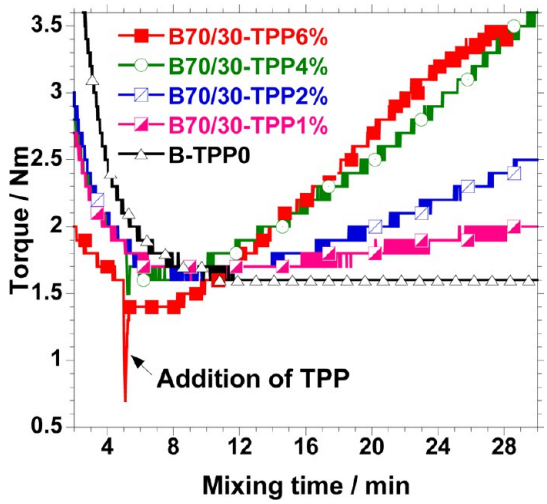

Figure 3. Torque as a function of the mixing time and TPP content.

hydroxyl and carboxyl end groups in the two polyesters. The higher proportion of PLA in the blend implied that the number of hydroxyl and carboxyl end groups that could take part in the reaction with TPP were more for the former than for the latter (for 70/30 blends), and hence more PLA−PLA linkages were expected. In any case, the viscosity of PBSA compared to that of PLA was very low and, as such, PLA−PBSA and PBSA−PBSA linkages may not have resulted in a significant increase in the viscosity, at least not on the same scale as PLA−PLA linkages.

Although the exact mechanism of such chain extension and chain interchange reactions, as promoted by TPP, is not precisely understood, two research groups[26,31] have put forward possible reaction paths. In the first case, the phosphorus atom from the TPP forms part of the extended chain,[26] while in the second case, only ester linkages from the polymers occur and the phosphorus atom does not form part of the extended polymer chain,[31] as shown in Scheme 1. To begin with, the hydroxyl end groups preferentially react with TPP by displacing one phenoxy group of the TPP. According to Jacques et al.,[31] the presence of three phenoxy functions allows the phosphite to undergo a multisubstitution process, with the equilibrium being displaced by phenol elimination, as shown in part A of Scheme 1. This substitution may go on until the phosphorus becomes a binding point, with the eventual possibility of chain branching (see product i in part A of Scheme 1). Conversely, Aharoni et al.[26] proposed a different reaction path, whereby, instead of subsequent substitution of the phenoxy groups by hydroxyl end groups, the carboxyl group reacts with the intermediate alkyl diphenyl phosphite, effectively resulting in chain extension, without the phosphorus atom being part of the chain (see product ii in Scheme 1). The byproduct in this reaction is diphenyl phosphite, which rearranges itself to the more thermodynamically stable diphenyl phosphate (DPP; see product iii). However, in both reaction paths, if the hydroxyl end groups are exhausted, the reaction between phosphites and the carboxyl group yields a phenyl ester at the end of the polymer chain (product iv) and DPP, as shown in Scheme 2. Regardless of the route of the reaction, chain extension and/or interchange do occur, and these lead to increased viscosity and, hence, increased torque values during reactive processing.

The byproducts of the compatibilization reaction (such as phenol) may, in the long run, negatively affect the molecular

dx.doi.org/10.1021/am400482f | ACS Appl. Mater. Interfaces 2013, 5, 4266−4276

Scheme 1. Reaction Mechanisms between Polyester Hydroxyl Chain Ends and Phosphite[26,31]

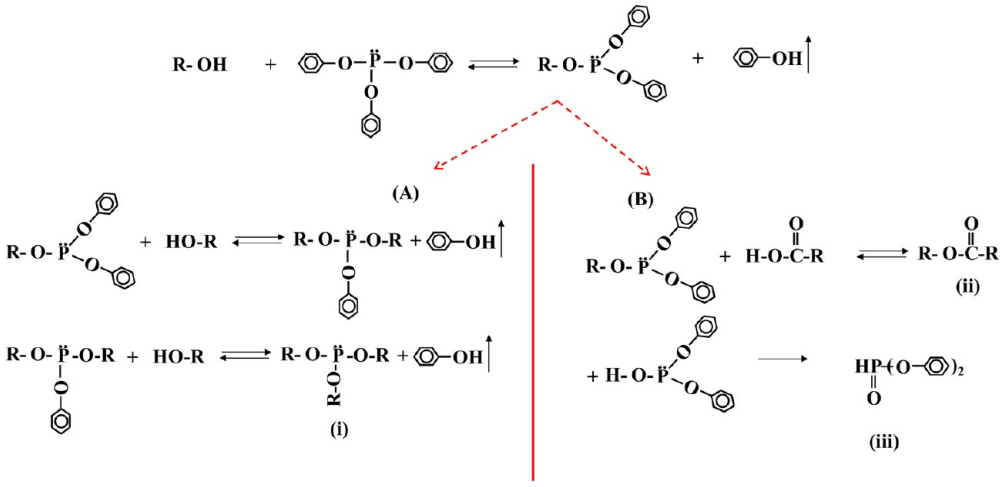

Scheme 2. Reaction Mechanisms between Polyester Carboxyl Chain Ends and Phosphite[26,31]

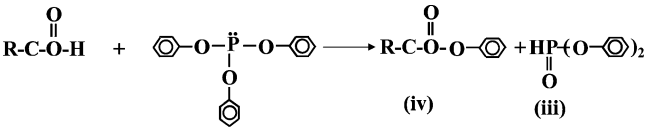

weight and mechanical properties of the blend. Continued mixing at elevated temperatures beyond a certain time leads to degradation of the blend and, hence, deterioration of properties. Although the graph is not shown here, the degradation was typified by a reduction in the torque values. At the same time, a complete transesterification process that results in random copolymers of PLA and PBSA may actually yield undesirable properties. It is important to note that, although analysis of the type of copolymer was not performed in this study, experimental results based on SEM observations and the optimization of various parameters to yield the desired mechanical properties suffice. Among the parameters optimized were the strategy/protocol of mixing, duration of mixing, concentration of TPP, and blend composition.

3.2. Processing Duration. There are two competing processes during mixing, namely, (i) chain extension and/or interchange and (ii) degradation. This is a disadvantage of using TPP to aid compatibilization because knowledge of the reaction kinetics would be necessary to precisely control the product formation. However, by following the torque/time graph, a fairly reasonable processing time may be determined within the region where chain extension and/or interchange are still dominant. Figure 4 shows the tensile properties of B70/30-TPP2% samples that had been processed at different times (8, 15, 30, and 40 min). The elongation-at-break increased steadily with time until it peaked in the region of 30 min, after which it drastically decreased. Although the modulus remained rather constant for samples processed within the 30 min processing window, it also drastically decreased for operations beyond this time. At higher processing times, i.e., 40 min, degradation reactions are dominant as a result of the chain scission initiated by byproducts such as phenol. Therefore, for 2 wt % TPP, the processing time was restricted to 30 min.

3.3. TPP Concentration. The effect of the TPP content on the tensile properties of previously annealed 70PLA/30PBSA blends is depicted in the graphs in Figure 5. Three independent

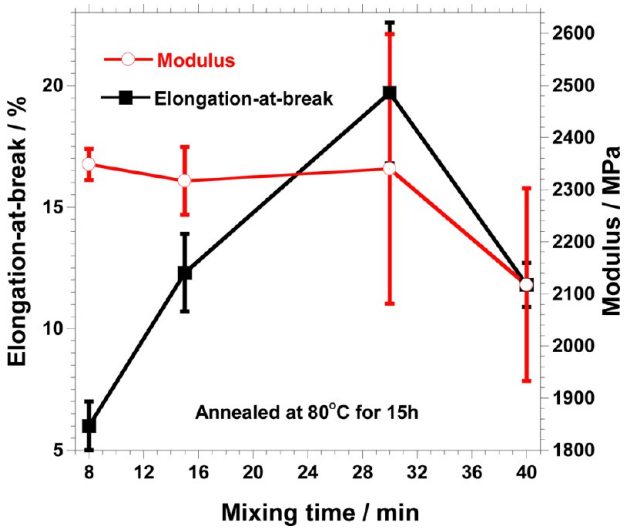

Figure 4. Effect of the processing time on the tensile properties of the B70/30-TPP2% blend.

tests were carried out to obtain the averages, with standard deviations being used as error bars. A 2 wt % TPP concentration was optimal because the highest improvement in the elongation-at-break was realized, and no loss in the modulus and tensile strength was observed. Although the effect of the TPP content on blends with other compositions is not shown here, 2 wt % TPP was also found to be optimal for the 90/10 blend. However, no attempt was made at optimizing the content of TPP for the 60/40 and 50/50 PLA/PBSA blend compositions because of their very poor morphologies. For the compatibilized 70/30 blend, there was a more than 3-fold increase in the elongation-at-break from 6 to 19.7% when 2% TPP was used in the compatibilization of the blend (see Figure 5). In a previous work,[18] the elongation-at-break for a similarly processed and annealed PLA sample was only 4%. Therefore, compatibilization resulted in a significant enhancement of the elongation-at-break of the brittle PLA.

Beyond 2% TPP concentration, there was a drastic reduction in the modulus and tensile strengths of the samples, while there was no change in the elongation-at-break. This result can be attributed to plasticization from the excess TPP or byproducts such as biphenyl phosphite or the stable DPP. It is worth

dx.doi.org/10.1021/am400482f | ACS Appl. Mater. Interfaces 2013, 5, 4266−4276

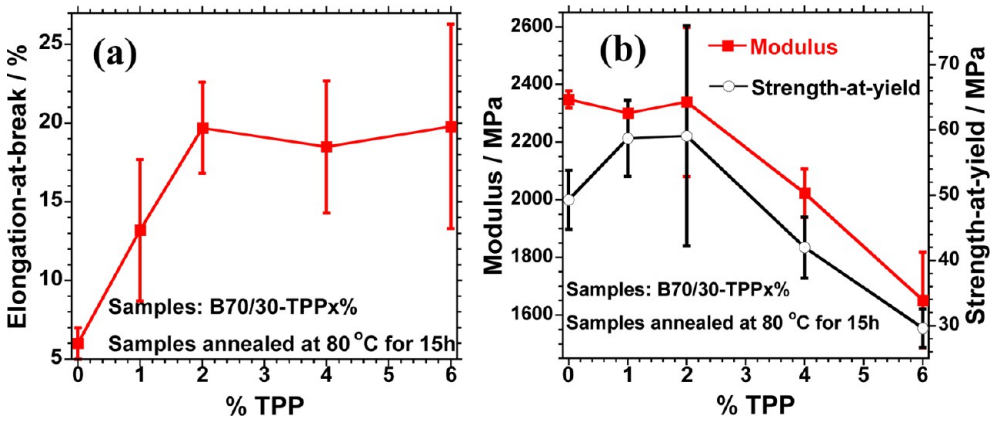

Figure 5. Effect of the TPP content on the tensile properties of compatibilized blends.

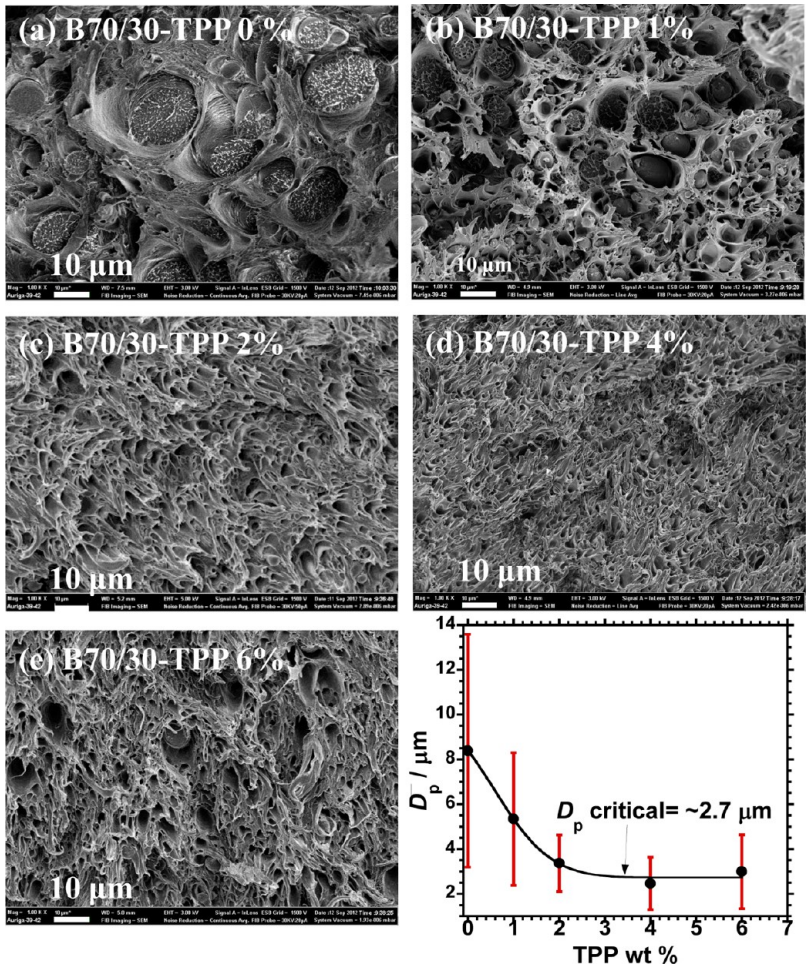

Figure 6. SEM images of (a) the neat B70/30 blend and blends compatibilized with different quantities of TPP. The graph shows the average diameter of the dispersed phase as a function of TPP. All of the samples were annealed at 80 °C for 15 h before imaging the tensile-fractured surfaces.

noting that, for a given polymer blend with a particular number-average molecular weight, there exist a number of hydroxyl and carboxyl end groups that participate in the chain elongation and compatibilization reaction at the start of reaction. Therefore, a given quantity of TPP molecules is needed to participate in the reactions. Beyond the required number of TPP molecules, the excess TPP would only plasticize the polymer blend, thus lowering the strength and modulus to unacceptable levels.

Tensile-fractured surfaces of the blends with different amounts of TPP were examined using SEM, and the results are shown in Figure 6. The roughness, depicted by the presence of fibrils and the lack of smoothness of the tensile-fractured surfaces, indicates that the deformation was by yield and hence ductile (rather than brittle) fracture, which is associated with PLA. Part f of Figure 6 shows a plot of the diameter of PBSA domains as a function of the TPP content. The number-average diameter of the PBSA domain was determined by the image

dx.doi.org/10.1021/am400482f | ACS Appl. Mater. Interfaces 2013, 5, 4266−4276

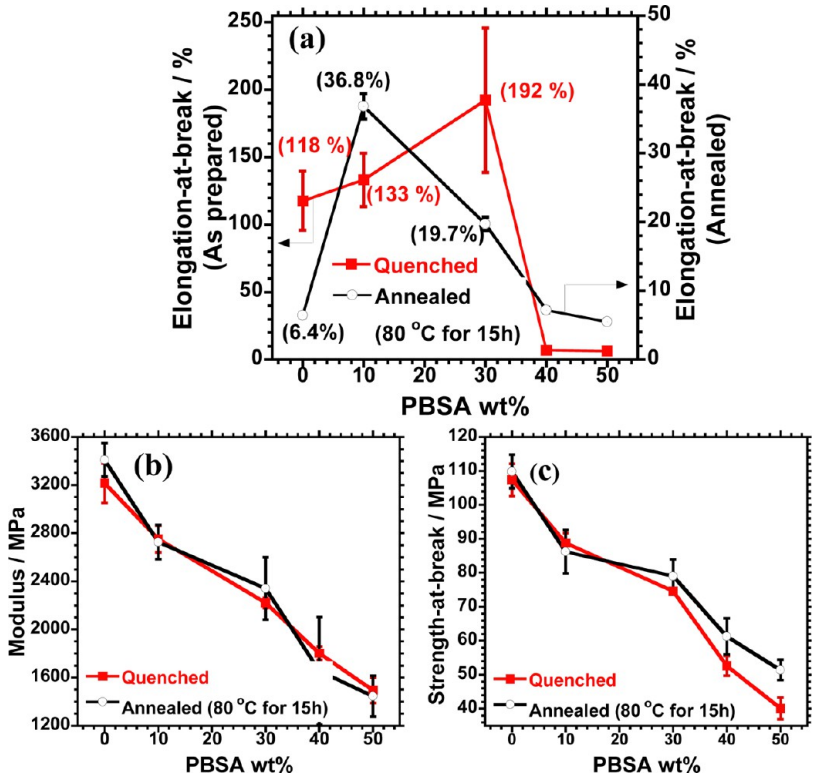

Figure 7. Tensile properties of neat PLA and compatibilized blends with various PBSA concentrations.

processing software, *ImageJ* (NIH, USA), using the following equation:

$$D_p = \frac{\sum n_i D_i}{\sum n_i} \quad (1)$$

where n_i is the number of the dispersed domains with diameter D_i counted from the SEM images.

The adhesion between PLA and PBSA was poor in the neat blend, as shown by the large dispersed-phase sizes. However, it improved to a more uniform morphology with the addition of TPP. As the TPP content was increased, there was a reduction in the PBSA domain size from an average of approximately 8 μm to a critical size of ~2.7 μm, below which no further reduction was observed. This critical size was obtained in the blend with approximately 2% TPP, further underscoring the fact that it was the optimal concentration.

3.4. Effect of the PLA/PBSA Composition. To study the tensile properties of compatibilized blends, two sample types were tested: (i) samples that had been annealed at 80 °C for 15 h; (ii) samples that had been quenched just after compression molding to keep PLA in an amorphous state, described as "as-prepared" samples. Both types of samples were used to study the effect of crystallinity (annealing) on the tensile properties. The tensile properties of neat PLA and compatibilized blends with various PBSA concentrations are shown in Figure 7. To appreciate the nature of failure occurring in the compatibilized blends while under tension, typical stress/strain graphs were plotted for selected samples, as shown in Figure 8.

As shown in Figure 7a, the quenched samples were not very useful in evaluating the effect of compatibilization on the elongation-at-break because even amorphous PLA had quite a high ductility, as expected. However, PBSA concentrations of over 30% resulted in extreme deterioration in properties, and

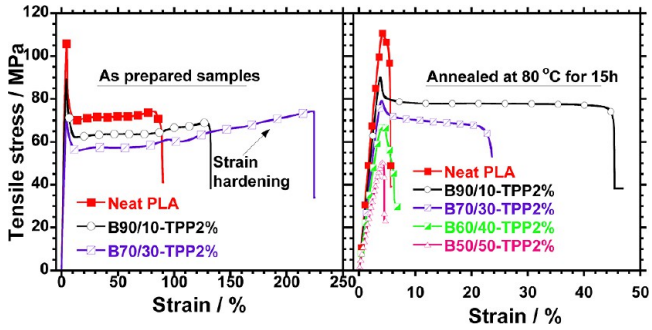

Figure 8. Typical stress/strain curves for (a) selected samples tested as prepared without annealing and (b) annealed neat PLA compatibilized blends of various compositions. The as-prepared samples were quenched immediately after compression molding to ensure that they were amorphous.

this was attributed to the poor morphology, as shown in parts c′ and d′ of Figure 1. Conversely, for the annealed samples, the elongation-at-break peaked at 36.6% for the B90/10-TPP2% sample, even though the 19.7% elongation-at-break for B70/30-TPP2% was also quite an improvement for the brittle PLA.

The moduli and tensile strengths of the compatibilized blends decreased with increased PBSA concentration, as expected. More importantly, the difference between annealed and "as-prepared" samples was not noticeable, save for the tensile strength of blends with higher PBSA concentration. Annealing the blends at 80 °C for 15 h crystallized the PLA phase (data not presented here), leading to worsened phase separation in neat blends that had poorer interfacial adhesion. However, the improved interfacial adhesion as a result of compatibilization prevented phase separation, and hence only

dx.doi.org/10.1021/am400482f | ACS Appl. Mater. Interfaces 2013, 5, 4266−4276

marginal differences between the moduli and tensile strengths of annealed and quenched samples were observed.

In Figure 8b, typical stress/strain curves show that PLA and compatibilized PLA/PBSA blends with poor phase morphologies, B50/50-TPP2% and B60/40-TPP2%, had brittle failure. Conversely, ductile failure was evident for compatibilized blends (B90/10-TPP2% and B70/30-TPP2% blends) that had somewhat uniform morphologies. The yield stress in PLA was quite high compared to that of the compatibilized blends. The lowering of the yield stress in the blends was as a result of the stress released after debonding that was caused by the previously concentrated stress in the PBSA phase during tensile pull. Because of the lowered stress, the major matrix (PLA) was allowed to yield slowly, hence the toughening in the B90/10-TPP2% and B70/30-TPP2% blends. However, for the B50/50-TPP2% and B60/40-TPP2% blends, poor interfacial adhesion caused premature debonding, which led to early propagation of the void and hence brittle failure. More discussion on the effect of the blend composition is in the Resistance to Impact section.

3.5. Resistance to Impact. Figure 9 shows the notched Charpy impact strength of neat PLA, the neat B70/30 blend,

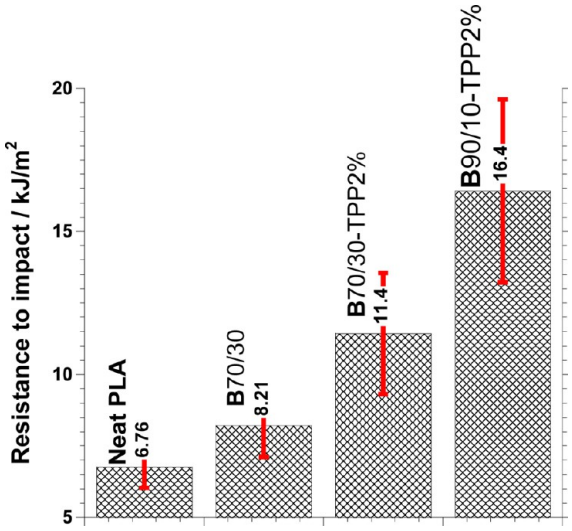

Figure 9. Impact strength of neat PLA, the 70PLA/30PBSA blend, and the compatibilized blends of PLA and PBSA at two compositions. The figure shows the average values of resistance to impact, obtained after six tests were carried out.

and the compatibilized blends at two compositions, B70/30-TPP2% and B90/10-TPP2%. Six independent tests were carried out, and the average values obtained are shown in the bar graph. Because crystallinity adversely affects the impact strength of the blends, the samples were initially annealed at 80 °C for 15 h to present a worst-case scenario. Although there was a slight increase in resistance to impact when PBSA was added to PLA, a significant increase in toughness was only realized after compatibilization, as initiated by TPP. The impact strength of PLA rose from 6 kJ/m^2 to 11 and 16 kJ/m^2 for B70/30-TPP2% and B90/10-TPP2%, respectively.

The tensile toughening mechanism in the polymer blends was ascribed to the yielding deformation of the matrix, as exemplified by the fibrils shown in the SEM images in Figures 1 and 6. In the same breadth, the improved resistance to impact in the blends is attributed to shear yielding of the matrix, which had been initiated by debonding microvoids. In polymer blends, microvoiding is widely considered a necessary step that enables matrix shear yielding and hence dissipation of energy.[32−34] According to the model of micromechanical deformation in blends by Kim and Michler,[33] a three-stage process was envisaged: (i) stress concentration within the inclusion; (ii) void and shear band formation; (iii) induced shear yielding. Because PLA and PBSA exhibit different resistances to impact, with the latter being tougher, the PBSA particles could act as stress concentrators in the blends.[35] This essentially converts the uniaxial stress to a triaxially concentrated stress that leads to volume dilation around the PBSA particle. For the neat blend, debonding easily occurs because of poor adhesion between the phases. Conversely, for compatibilized blends, deformation occurs through a debonding process with fibrillated ligaments at the interface, such as the ones observed in Figure 1. The poor interfacial adhesion between PLA and PBSA in the neat blends led to premature interfacial failure and hence rapid void propagation, while the moderately good interfacial adhesion in the compatibilized blend delayed the occurrence of matrix deformation. In the compatibilized blends, greater applied energy is consumed for the above-mentioned processes, i.e., volume dilation, void initiation, and propagation, and hence more toughening is obtained compared to that of the neat blend. However, in both cases, the greatest energy dissipation occurs during the next stage in the deformation process, i.e., matrix yielding, which is initiated by the microvoids.

It has been argued that, for various compositions, the 70PLA/30PBSA blend resulted in the most tensile toughening because of the maximum specific interfacial area exposed by the PBSA phase to the PLA matrix.[18] However, for compatibilized blends, it was not possible to estimate the average PBSA domain sizes in the B90/10-TPP2% blend because they were too small. As such, it may be possible that the specific surface area exposed by the PBSA phase in the B90/10-TPP2% blend was higher than that in the B70/30-TPP2% blend. This, in turn, meant that the interfacial adhesion is better in the B90/10-TPP2% blend than in the B70/30-TPP2% blend and hence the higher impact resistance posted by the former sample.

It is a known fact that crystallinity and crystal size affect the mechanical properties of polymers and indeed their blends. Figure 10 shows the XRD diffractograms of the unmodified blends and TPP-modified blends. All quenched samples did not show any peak (hence, only the result for the neat blend is shown), thus indicating that they were completely amorphous. On the other hand, annealed samples showed characteristic PLA and PBSA crystalline peaks. The similarities in the peak positions for modified and unmodified blends signified that there was structural similarity between the crystals of unmodified and TPP-modified blends. Therefore, the difference in the mechanical properties between modified and unmodified blends could not be attributed to crystalline structure differences. In fact, as will be discussed later, TPP enhanced the crystallinity of the PLA component, which would have made it more brittle and not as ductile (and as tough) as was shown earlier. This reenforces the point that improved interfacial adhesion between PLA and PBSA, as a result of compatibilization with TPP, accounted for the observed improvement in impact and tensile toughness.

3.6. Thermal Properties. DSC and TGA were used to characterize the thermal properties of the neat and compatibilized blends. Typical DSC curves obtained during second

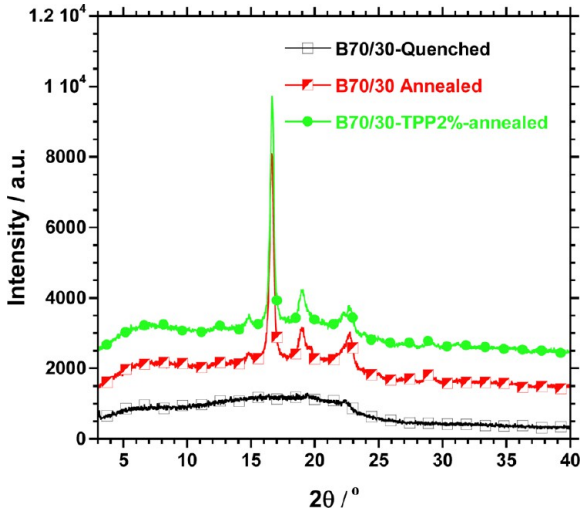

Figure 10. XRD patterns for a quenched unmodified B70/30 blend and annealed unmodified and TPP-modified B70/30 blends. Annealing was done at 80 °C for 15 h.

heating runs are shown in Figure 11. The curves were characterized by the cold crystallization temperature (T_{cc}) of

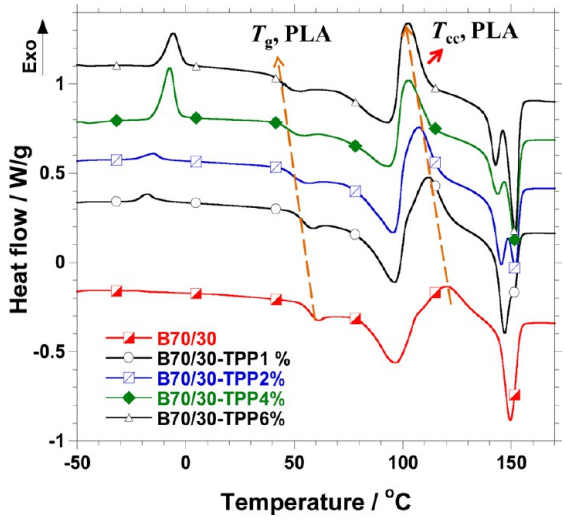

Figure 11. DSC second heating curves of the neat blend and compatibilized blends with different TPP contents.

PBSA, the T_g of PLA, the melting peaks of PBSA, the T_{cc} of PLA, and the melting peaks of PLA (T_m^1 and T_m^2). Of interest in the current study was the effect of the TPP content on the thermal properties of the blend, especially the PLA component. Three independent runs were carried out at a heating rate of 10 °C/min from −60 to +190 °C. The average values of T_g, T_{cc}, T_m, and the PLA component degree of crystallinity, X_c, are reported in Table 1.

T_g of PLA decreased at a slow rate from 58 to 45 °C with an increase in the TPP content from 0 to 6%. This was attributed to two factors: (i) compatibilization of PLA and PBSA, making the two partially miscible at the interface and, hence, pushing the PLA T_g toward that of PBSA; (ii) the plasticizer effect of TPP and some of the byproducts, such as DPP, of the compatibilization reactions. It has been shown that compounds such as triphenyl phosphate could act as a plasticizer of PLA.[8] Because of the depression in T_g of the PLA component, its crystallinity also increased from 26.6 to 39.5% with an increase in the TPP content from 0 to 6%. The improvement in crystallinity would imply an increase in the brittleness in the blend. However, as has been seen before, the addition of TPP actually enhanced the ductility of the blend, meaning that the effect of crystallinity on the mechanical properties was not as profound as the effect of improved interfacial adhesion, as a result of compatibilization.

The depression in T_g enhanced the flexibility of molecules at lower temperatures; hence, the cold crystallization onset and peak temperatures correspondingly decreased with an increase in the TPP content. Whereas the main melting point of PLA, T_m^2, remains constant at 151 °C regardless of the TPP content, the first melting point decreased with an increase in the TPP content. This was attributed to imperfect PLA crystal formation in the presence of TPP. The imperfect crystals with thinner lamella melted first, before recrystallizing and melting again at higher temperatures.

Cold crystallization of PBSA increased with an increase in the TPP content, and the peak shifted to higher temperatures. This implies that, during the cooling run, PBSA did not crystallize fully in blends with large quantities of TPP and had to crystallize upon heating. With increased compatibilization, the number of units of PBSA chains remaining free to join a crystallization fold during cooling was reduced or their motion was impaired, and hence only after reheating did they have sufficient energy to crystallize.

The thermal stabilities of neat and compatibilized blends and TPP were determined through thermoxidative analyses using TGA. Figure 12 is a plot of the relative weight losses as a function of the temperature. Only selected blends are shown for clarity: the neat blend and blends with optimal and maximum TPP contents. To compare the thermal stability of

Table 1. Average Thermal Properties of the PLA Component in Neat and Compatibilized Blends, As Obtained from DSC[a]

sample	T_g (°C)	T_{cc} (°C)	T_m^1 (°C)	T_m^2 (°C)	X_c[b] (%)
PLA	59 (0.2)		151 (0.2)		26.1 (0.1)
B70/30	58 (0.4)	121 (0.6)	149 (0.4)		26.6 (0.3)
B70/30-TPP1%	54 (1)	112 (0.6)	147 (0.2)	151 (0.2)	29.8 (0.5)
B70/30-TPP2%	50 (0.6)	109 (0.8)	146 (0.1)	152 (0)	30.0 (0.9)
B70/30-TPP4%	48 (1.4)	101 (1.8)	143 (0.5)	151(0.5)	33.3 (1.1)
B70/30-TPP6%	45 (1.2)	103 (0.9)	143 (0.7)	151 (0.4)	39.5 (0.5)

[a]The samples had been annealed at 80 °C for 15 h. [b]$X_c = \Delta H_m^{PLA}/93 \times 100$, where 93 was taken as the enthalpy of a pure PLA crystal (100% crystal).[36] The ΔH_m^{PLA} was obtained from the heat of fusion of the PLA component during the first heating cycle, whereas T_g, T_{cc}, and T_m were obtained from the second heating cycle. Three independent runs were performed and the average values reported. The standard deviations are shown in parentheses.

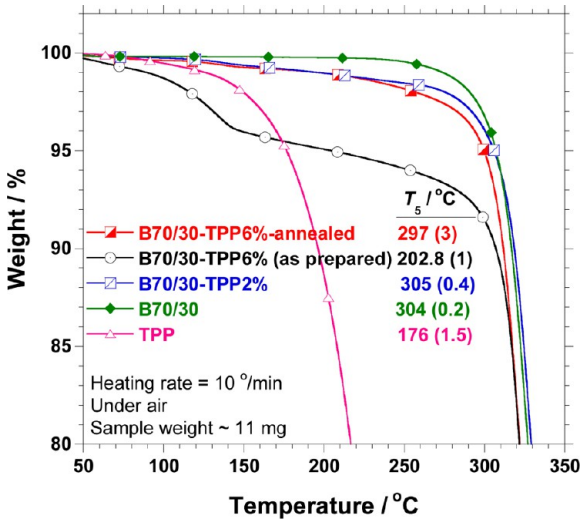

Figure 12. TGA traces of weight loss as a function of the temperature for selected blends and TPP. All of the blends were annealed at 80 °C for 15 h prior to degradation. The "as-prepared" B70/30-TPP6% blend was included to show the adverse effects of high TPP content. The figures in the graph indicate average T_5 values and their standard deviations. The T_5 values for blends with 1 and 4% of TPP are 302 (0.7) and 303 (1), respectively.

the samples, the onset degradation temperature, T_5, taken arbitrarily as the temperature at which 5% degradation occurred, was determined in three independent tests; the average values are tabulated in Figure 12.

From the curves, it is noted that the thermal stability of TPP is quite low, with T_5 being just 176 °C. It follows that if the quantity of TPP is sufficiently high, a significant portion will either remain unreacted or the byproducts formed would be sufficiently high to lower the thermal stability of the blends. As such, the quantity of TPP used needs to be minimal but effective to avoid its accumulation within the blend matrix. Indeed, for blends with TPP loadings of up to 4 wt %, the T_5 values were not significantly different from those of the neat blend. However, for higher values of TPP, there was a notable reduction in the thermal stability, as seen in Figure 12.

To clearly illustrate the adverse effect of high TPP content on thermal stability, an "as-prepared" B70/30-TPP6% sample was thermally degraded without prior annealing. A drastic reduction in the thermal stability was observed, with T_5 being 203 °C. This reduction was due to the presence of either unreacted TPP or byproducts that accumulated within the blend matrix. However, upon annealing, TPP and/or byproducts of the compatibilization reaction such as DPP vaporized; hence, the thermal stability improved, with T_5 increasing to 297 °C.

In conclusion, the content of TPP should be kept low enough to prevent it, or the resultant compatibilization byproducts, from accumulating. For high concentrations, for instance, 6 wt % as in the current study, the thermal stability of the blend is severely compromised. For less adverse effects on the thermal stability, a TPP concentration of approximately 2 wt % is considered optimal. In addition, reactive compatibilization of the blends in the presence of organomodified clay led to a tremendous improvement in the thermal stability; this aspect will be discussed in a separate paper.

4. CONCLUSIONS

Toughened biodegradable PLA and PBSA blends were successfully prepared by melt mixing in the presence of TPP to enhance in situ compatibilization. The resultant compatibilized blends showed improved toughness, depending on the quantities of TPP and PBSA and the sequence and duration of mixing. As a result of compatibilization and enhanced intraphase viscosity during processing, the morphology of blends improved from the two-phase island-sea type to a more uniform blend. The improvement in resistance to impact and elongation-at-break was attributed to yielding deformation in the matrix, as initiated by the debonding between PLA/PBSA phases.

Although TPP has low thermal stability, as long as the concentration was not above 2 wt %, there was no noticeable reduction in the thermal stability. However, high concentrations must be avoided because of the possibility of TPP accumulating within the blend matrix, thus having detrimental effects on the thermomechanical properties.

In conclusion, it has been shown that the problem of PLA brittleness may be solved through blending with PBSA in the presence of TPP, in a reactive compatibilization process. Incorporation of clay into such a system may yield not only improved mechanical and thermal properties but also reduced permeability.

AUTHOR INFORMATION

Corresponding Author

*Fax: +2712841 2229. E-mail: rsuprakas@csir.co.za.

Notes

The authors declare no competing financial interest.

ACKNOWLEDGMENTS

S.S.R. and V.O. thank the Technology Innovation Agency, Council for Scientific and Industrial Research, Department of Science and Technology, and National Research Foundation, South Africa, for financial support.

REFERENCES

(1) Van de Velde, K.; Kiekens, P. *Polym. Test.* **2002**, *21*, 433.
(2) Sinha Ray, S. *Acc. Chem. Res.* **2012**, *45*, 1710.
(3) Broz, M. E.; VanderHart, D. L.; Washburn, N. R. *Biomaterials* **2003**, *24*, 4181.
(4) Chen, C.-C.; Chueh, J.-Y.; Tseng, H.; Huang, H.-M.; Lee, S.-Y. *Biomaterials* **2003**, *24*, 1167.
(5) López-Rodríguez, N.; López-Arraiza, A.; Meaurio, E.; Sarasua, J. R. *Polym. Eng. Sci.* **2006**, *46*, 1299.
(6) Todo, M.; Park, S. D.; Takayama, T.; Arakawa, K. *Eng. Fract. Mech.* **2007**, *74*, 1872.
(7) Odent, J.; Raquez, J.-M.; Duquesne, E.; Dubois, P. *Eur. Polym. J.* **2012**, *48*, 331.
(8) Odent, J.; Leclère, P.; Raquez, J.-M.; Dubois, P. *Eur. Polym. J.* **2013**, *49*, 914.
(9) Jiang, L.; Wolcott, M. P.; Zhang, J. *Biomacromolecules* **2005**, *7*, 199.
(10) Gu, S.-Y.; Zhang, K.; Ren, J.; Zhan, H. *Carbohyd. Polym.* **2008**, *74*, 79.
(11) Xiao, H.; Liu, F.; Jiang, T.; Yeh, J.-T. *J. Appl. Polym. Sci.* **2010**, *117*, 2980.
(12) Zhao, Q.; Wang, S.; Kong, M.; Geng, W.; Li, R. K. Y.; Song, C.; Kong, D. *J. Biomed. Mater. Res. B: Appl. Biomater.* **2011**, *100B*, 23.
(13) Zhang, K.; Mohanty, A. K.; Misra, M. *ACS Appl. Mater. Interfaces* **2012**, *4*, 3091.

(14) Han, L.; Han, C.; Zhang, H.; Chen, S.; Dong, L. *Polym. Compos.* **2012**, *33*, 850.
(15) Park, J. W.; Im, S. S. *J. Appl. Polym. Sci.* **2002**, *86*, 647.
(16) Shibata, M.; Inoue, Y.; Miyoshi, M. *Polymer* **2006**, *47*, 3557.
(17) Liu, X.; Dever, M.; Fair, N.; Benson, R. *J. Polym. Environ.* **1997**, *5*, 225.
(18) Ojijo, V.; Sinha Ray, S.; Sadiku, R. *ACS Appl. Mater. Interfaces* **2012**, *4*, 6690.
(19) Ojijo, V.; Cele, H.; Ray, S. S. *Macromol. Mater. Eng.* **2011**, *296*, 865.
(20) Ojijo, V.; Malwela, T.; Sinha Ray, S.; Sadiku, R. *Polymer* **2012**, *53*, 505.
(21) Ojijo, V.; Sinha Ray, S.; Sadiku, R. *ACS Appl. Mater. Interfaces* **2012**, *4*, 2395.
(22) van Aert, H. A. M.; van Steenpaal, G. J. M.; Nelissen, L.; Lemstra, P. J.; Liska, J.; Bailly, C. *Polymer* **2001**, *42*, 2803.
(23) Tuba, F.; Oáh, L.; Nagy, P. t. *Eng. Fract. Mech.* **2011**, *78*, 3123.
(24) Harada, M.; Iida, K.; Okamoto, K.; Hayashi, H.; Hirano, K. *Polym. Eng. Sci.* **2008**, *48*, 1359.
(25) Coltelli, M.-B.; Toncelli, C.; Ciardelli, F.; Bronco, S. *Polym. Degrad. Stab.* **2011**, *96*, 982.
(26) Aharoni, S. M.; Forbes, C. E.; Hammond, W. B.; Hindenlang, D. M.; Mares, F.; O'Brien, K.; Sedgwick, R. D. *J. Polym. Sci., Polym. Chem* **1986**, *24*, 1281.
(27) Cavalcanti, F. N.; Teófilo, E. T.; Rabello, M. S.; Silva, S. M. L. *Polym. Eng. Sci.* **2007**, *47*, 2155.
(28) Dias, M. L.; Silva, A. P. F. *Polym. Eng. Sci.* **2000**, *40*, 1777.
(29) Wang, L.; Ma, W.; Gross, R. A.; McCarthy, S. P. *Polym. Degrad. Stab.* **1998**, *59*, 161.
(30) Scaffaro, R.; Mistretta, M. C.; La Mantia, F. P.; Gleria, M.; Bertani, R.; Samperi, F.; Puglisi, C. *Macromol. Chem. Phys.* **2006**, *207*, 1986.
(31) Jacques, B.; Devaux, J.; Legras, R.; Nield, E. *Polymer* **1997**, *38*, 5367.
(32) Liu, H.; Song, W.; Chen, F.; Guo, L.; Zhang, J. *Macromolecules* **2011**, *44*, 1513−1522.
(33) Kim, G. M.; Michler, G. H. *Polymer* **1998**, *39*, 5699.
(34) Kim, G. M.; Michler, G. H. *Polymer* **1998**, *39*, 5689.
(35) Wang, R.; Wang, S.; Zhang, Y.; Wan, C.; Ma, P. *Polym. Eng. Sci.* **2009**, *49*, 26.
(36) Tsuji, H.; Ikada, Y. *Polymer* **1995**, *36*, 2709.